

# A study of the soft X-ray photoreduction of $[\text{Ni}^{\text{IV}}(\text{S}_2\text{CNET}_2)_3][\text{BF}_4]$ and soft X-ray photoisomerisation of $[\text{PPh}_4][\text{Ni}^{\text{II}}(\text{S}_2\text{COEt})_3]$ at the Ni L-edge †

David Collison,<sup>c</sup> C. David Garner,<sup>c</sup> Catherine M. McGrath,<sup>a</sup> J. Frederick W. Mosselmans,<sup>b</sup> Elna Pidcock,<sup>c</sup> Mark D. Roper,<sup>b</sup> Barry G. Searle,<sup>b</sup> Jon M. W. Seddon,<sup>a</sup> Ekk Sinn<sup>a</sup> and Nigel A. Young<sup>a\*</sup>

<sup>a</sup> Department of Chemistry, The University of Hull, Hull, UK HU6 7RX.

E-mail: n.a.young@chem.hull.ac.uk

<sup>b</sup> CCLRC Daresbury Laboratory, Daresbury, Warrington, Cheshire, UK WA4 4AD

<sup>c</sup> Department of Chemistry, The University of Manchester, Oxford Road, Manchester, UK M13 9PL

Received 22nd July 1998, Accepted 27th October 1998

A detailed study of the soft X-ray photochemistry occurring in some nickel dithiocarbamate and xanthate complexes has shown that soft X-ray induced photoreduction of  $[\text{Ni}^{\text{IV}}(\text{S}_2\text{CNET}_2)_3][\text{BF}_4]$  results in a  $\text{Ni}^{\text{II}}$  square-planar species and the rate is dependent on photon flux, photon energy and ligand set, but is essentially independent of temperature. Also, it has been demonstrated that  $[\text{PPh}_4][\text{Ni}^{\text{II}}(\text{S}_2\text{COEt})_3]$  is photoisomerised to a  $\text{Ni}^{\text{II}}$  square-planar species on exposure to soft X-rays. The implication for experiments on third generation synchrotron sources is discussed briefly.

Although the chemistry of transition metal dithiocarbamate and xanthate, xan, (or dithiocarbonate, abbreviated as dtc) complexes has been extensively studied, the characterisation of the electronic structure of these often intensely coloured metal complexes by UV/VIS spectroscopy can be hampered by intense charge transfer (CT) bands. This has encouraged us to investigate the applicability of 3d L-edge X-ray absorption fine structure (XAFS) spectroscopy to the study of electronic structure in these and a wide range of other complexes.<sup>1-3</sup>  $L_{2,3}$ -edge X-ray absorption spectra arise from the excitation of 2p electrons, and in the case of the 3d transition metals the spectra are dominated by intense dipole allowed  $2p^63d^n \rightarrow 2p^53d^{n+1}$  transitions. Whilst  $2p \rightarrow 4s$  transitions are also dipole allowed, they only have about 1/30th of the intensity of the  $2p \rightarrow 3d$  transitions due to the large overlap of the 3d and 2p wavefunctions compared to that of the 2p and 4s.<sup>4</sup> The strong interaction between the 2p core-hole and the valence 3d orbitals means that the element specific spectra are very sensitive to oxidation state, spin state, ligand field and local environment.<sup>5</sup> The natural line-widths at the  $L_{2,3}$ -edges of the 3d metals are of the order of 0.5 eV<sup>6</sup> (about a quarter of the value at the corresponding K-edges), therefore the fine structure can be used to obtain detailed information about the electronic structure, especially for  $d^0$  systems and where the d-d transitions are masked by charge transfer bands in optical spectra. Although a relatively recent development,  $L_{2,3}$ -edge XAFS has been applied to the study of minerals, metalloproteins and coordination compounds<sup>7</sup> as well as solid state physics and chemistry.<sup>8</sup> Previous Ni L-edge XAFS studies<sup>3,4,9-23a</sup> have indicated that the different  $2p^63d^n \rightarrow 2p^53d^{n+1}$  transitions which arise from different oxidation states and geometries, manifest themselves as: (i) shifts in energy of the L-edge features (due to changes both in the 2p binding energy, and the energy difference between the 2p core-hole and the empty 3d orbitals); (ii) changes in the widths of the  $L_3$  and  $L_2$  peaks (due to the number of allowed transitions); (iii) changes in the branching ratio

$\{I(L_3)/[I(L_3) + I(L_2)]\}$  (which are related to the degeneracy and spin states of the ground and excited states).<sup>11,13,20,24</sup> In general, a higher formal oxidation state of the metal results in a shift of the  $L_3$  and  $L_2$  features to higher energy (due to the larger 2p binding energy), and an increase in the integrated peak intensity (due to the change in the number of holes in the d-manifold). In addition to changes in geometry and oxidation state, the extent of covalency in the system can also considerably affect the spectra, with an increase in the covalency of the metal-ligand bonding generally resulting in the 'smearing out' of structure on both the  $L_3$  and  $L_2$  peaks.

We have recently observed<sup>1</sup> two soft X-ray induced photochemical processes occurring in  $[\text{Fe}(\text{phen})_2(\text{NCX})_2]$ , (phen = 1,10-phenanthroline, X = S, Se). One of these is the reversible conversion of a low-spin state into a meta-stable high-spin state at low temperature (<55 K), and we have described this as soft X-ray induced excited spin state trapping (SOXIESST), analogous to the processes known as LIESST<sup>25</sup> or NIESST<sup>26</sup> where visible light or nuclear decay can also result in the formation of meta-stable high spin states at low temperature. The other photochemical process results in the transformation of either high- or low-spin  $[\text{Fe}(\text{phen})_2(\text{NCX})_2]$  to a low-spin species that cannot be converted to a high-spin state by either further irradiation or temperature cycling, and we have described this process as soft X-ray photochemistry (SOXPC). The rate of SOXIESST is much greater than that for SOXPC, and the rate of SOXPC is dependent on spin-state and ligand set. We report here a further detailed study of soft X-ray photochemistry (SOXPC) arising from irradiation of  $[\text{PPh}_4][\text{Ni}^{\text{II}}(\text{S}_2\text{COEt})_3]$  and of  $[\text{Ni}^{\text{IV}}(\text{S}_2\text{CNET}_2)_3][\text{BF}_4]$  at the Ni L-edge.

## Experimental

### Sample preparation

Bis(*N,N*-diethyldithiocarbamato)nickel(II)  $[\text{Ni}^{\text{II}}(\text{S}_2\text{CNET}_2)_2]$ ,<sup>27</sup> tris(*N,N*-diethyldithiocarbamato)nickel(IV) tetrafluoroborate  $[\text{Ni}^{\text{IV}}(\text{S}_2\text{CNET}_2)_3][\text{BF}_4]$ ,<sup>28</sup> tris(*N,N*-di-*n*-butyldithiocarbamato)nickel(IV) tetrafluoroborate  $[\text{Ni}^{\text{IV}}(\text{S}_2\text{CN}^n\text{Bu}_2)_3][\text{BF}_4]$ ,<sup>28</sup> bis(ethyl-xanthato)nickel(II)  $[\text{Ni}^{\text{II}}(\text{S}_2\text{COEt})_2]$ <sup>29</sup> and tetraphenylphos-

† Soft X-ray photochemistry at the  $L_{2,3}$ -edges of 3d transition metal complexes, Part 2.<sup>1</sup>

phonium tris(ethylxanthato)nickelate(II)  $[\text{PPh}_4][\text{Ni}^{\text{II}}(\text{S}_2\text{COEt})_3]$ <sup>30</sup> were synthesised by literature methods. Elemental analysis (C,H,N,S) of all species, NMR (<sup>1</sup>H, <sup>13</sup>C) spectroscopy of all ligands and diamagnetic complexes and electrospray mass spectrometry of selected species were satisfactory.

### Soft X-ray absorption measurements

The samples for Ni and S L-edge XAFS spectroscopy were mounted on Al-coated Ni stubs as freshly ground powders on double sided carbon tape (Agar Products, Cambridge, UK) in a nitrogen purged glove bag. The stubs were transferred anaerobically to the load-lock of the UHV sample chamber *via* a desiccator and nitrogen purged glove bag to avoid aerial contamination of the surfaces. Soft X-ray absorption spectra were measured on station 5U.1 of the undulator beamline<sup>31</sup> at the Daresbury Laboratory Synchrotron Radiation Source (SRS) operating at 2 GeV with circulating currents in the range 100–250 mA and lifetimes of 12–24 h. Total electron yield (TEY) detection was used both in the drain current and channeltron modes, giving an estimated sampling depth of 30–50 Å. The drain current mode gave consistently higher quality data (in terms of signal to noise ratio) but the channeltron mode was used during variable temperature (VT) work so that the temperature sensor could be attached directly to the sample stage. The estimated photon flux at the sample was *ca.*  $10^{11}$  photons  $\text{s}^{-1}$  and this decreased by about a factor of two over the beam lifetime. The photon flux also varied between experimental runs, due to modifications and improvements in the beamline, resulting in a variation of focal spot size at the sample; typical dimensions were of the order of  $1 \times 1.5$  mm<sup>2</sup>. The minimum measured experimental bandwidth (fwhm) of *ca.* 1.0 eV compared favourably with the convolution of the calculated optimum beamline resolution at 850 eV (with 50  $\mu\text{m}$  slits) of *ca.* 0.6 eV and the Ni L-edge core-hole lifetime of *ca.* 0.5 eV.<sup>6</sup> In order to exclude visible light, all viewports were kept covered with several layers of Al foil in addition to plastic port covers and a cold cathode (Penning) gauge was used to monitor the pressure. Furthermore, no differences were observed in the spectra when the optically transparent polycarbonate (Lexan) contamination barrier between the beamline and the UHV sample chamber was replaced by a thin optically opaque aluminium window (maximum visible transmittance  $5 \times 10^{-8}$ ) thus excluding the possibility of any scattered visible light from the beamline reaching the sample. The Ni L-edge spectra were not corrected with respect to beam decay using  $I/I_0$  due to the presence of an NiO impurity in the  $I_0$  channel (which had no effect on the signal channel); instead they were background subtracted using a multi-fit line (Grams/32, Galactic Industries Corporation) and normalised to the  $L_3$  intensity maximum. The NiO impurity in the  $I_0$  channel facilitated an internal calibrant for each spectrum, using the maximum of the NiO  $L_3$  peak at 853.2 eV.<sup>10</sup> This internal *in situ* calibration method allows for very accurate determination of peak positions ( $\pm 0.1$  eV) and hence gives a high level of confidence in identifying subtle changes between spectra. In order to be able to make meaningful comparisons between experiments carried out during the different visits to the SRS over the period of *ca.* a year, an appropriate experimental protocol had to be developed as the photon flux and photon density delivered to the sample varied due to changes in the configuration of the beamline. Hence, comparison was only strictly consistent within each experimental run and also for experiments carried out with similar beam currents in the storage ring. For example, a full scan at the Ni L-edge typically took 24 minutes; therefore, irradiation experiments were carried out for this length of time and then a Ni L-edge spectrum was recorded, and compared with a second scan obtained from sequential scanning of a fresh sample. This procedure resulted in each sample being irradiated for the same total time. Peak deconvolution was carried out using Voigt profiles within

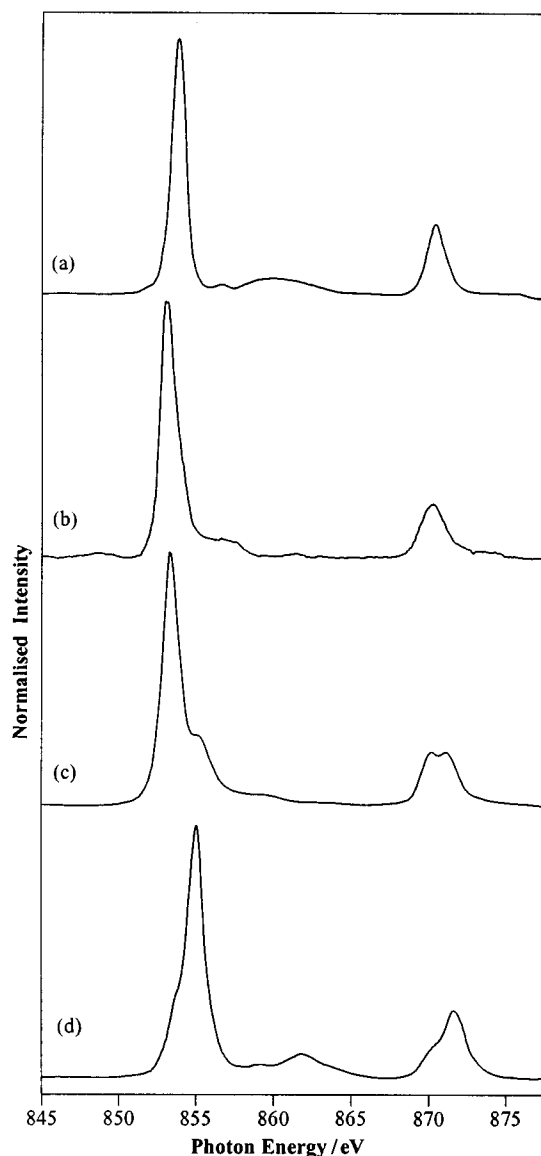


**Fig. 1** Ni L-edge spectra of (a)  $[\text{Ni}^{\text{II}}(\text{S}_2\text{CNEt}_2)_2]$ , (b)  $[\text{PPh}_4][\text{Ni}^{\text{II}}(\text{S}_2\text{COEt})_3]$ , (c)  $\text{NiS}_2$ , (d)  $[\text{Ni}^{\text{IV}}(\text{S}_2\text{CNEt}_2)_3][\text{BF}_4]$ .

Grams/32 and fitting of the kinetic data was accomplished using Solver and Solver Statistics<sup>32</sup> within Excel (Microsoft). Visible photochemistry was carried out with a 200W LOT-Oriel Hg–Xe lamp and Ealing Optics hot filter (400–700 nm band pass). Full details of the L-edge XAFS apparatus and experimental procedure have been published previously.<sup>1</sup>

## Results

### Nickel(II) complexes

Fig. 1(a) and (b) compare the spectra observed for  $[\text{Ni}^{\text{II}}(\text{S}_2\text{CNEt}_2)_2]$  and  $[\text{PPh}_4][\text{Ni}^{\text{II}}(\text{S}_2\text{COEt})_3]$ , respectively. The spectra are split into  $L_3$  ( $2p_{3/2}$ ) and  $L_2$  ( $2p_{1/2}$ ) components by spin–orbit coupling of the 2p core–hole (*ca.* 16 eV for Ni), and the structure on the higher energy  $L_2$  feature is less well resolved due to interaction with the  $L_3$  continuum states.<sup>5</sup> For  $[\text{Ni}^{\text{II}}(\text{S}_2\text{CNEt}_2)_2]$ , which is known to be square-planar,<sup>33</sup> the  $L_3$  maximum was at 853.8 eV with the  $L_2$  maximum at 870.4 eV. Associated with the  $L_3$  feature was a small peak at 856.6 eV, which has previously been shown to be associated with the coupling of the 2p core–hole to the  $b_2$ ,  $a_2$  and  $e$  3d orbitals.<sup>11,19</sup> The broad satellite feature at 859.7 eV has previously been identified to be due to differences in covalency of the initial and final states,<sup>19,34</sup> although more recently these bands have been assigned to be

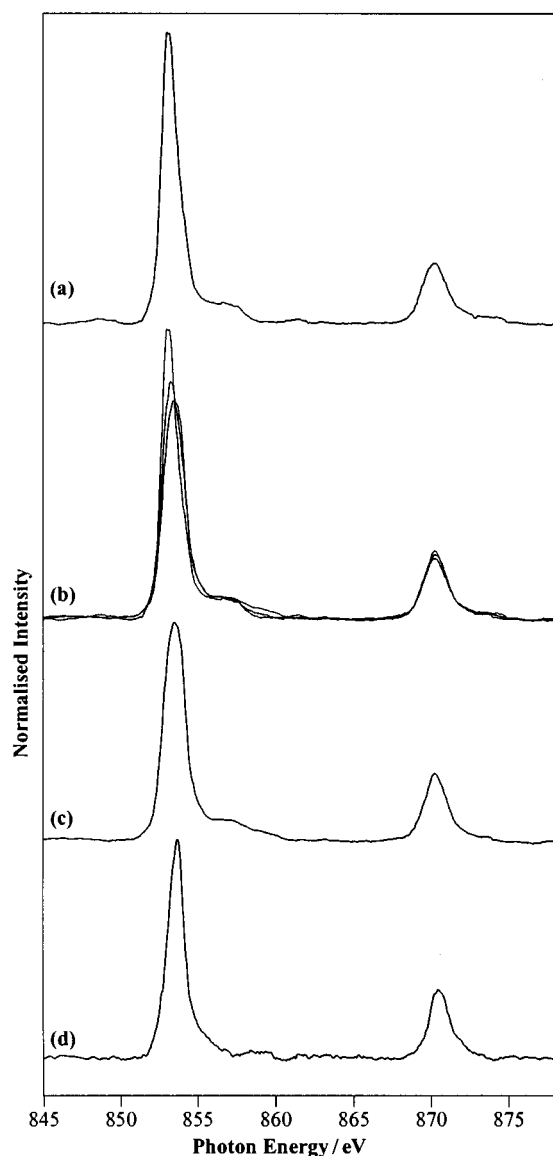


Fig. 2 Ni L-edge spectra of  $[\text{PPh}_4][\text{Ni}^{\text{II}}(\text{S}_2\text{COEt})_3]$ , (a) initial 25 min spectrum, (b) successive spectra, (c) final spectrum, (d)  $[\text{Ni}^{\text{II}}(\text{S}_2\text{COEt})_2]$ .

due to charge-transfer transitions,<sup>23a</sup> but still related to the extent of covalency in the metal–ligand bonding as shown by the spectra of  $\text{K}_2[\text{Ni}(\text{CN})_4] \cdot \text{H}_2\text{O}$  and  $[\text{Ni}(\text{Hdmg})_2]$  (Hdmg = dimethylglyoximate).<sup>23a</sup> The spectrum of  $[\text{Ni}^{\text{II}}(\text{S}_2\text{COEt})_2]$  [Fig. 2(d)] was essentially identical to that of  $[\text{Ni}^{\text{II}}(\text{S}_2\text{CNET}_2)_2]$  with the  $L_3$  and  $L_2$  maxima at 853.7 and 870.5 eV, respectively. The spectrum of  $[\text{PPh}_4][\text{Ni}^{\text{II}}(\text{S}_2\text{COEt})_3]$  [Fig. 1(b)], which is pseudo-octahedral but with considerable distortion due to the acute chelate bite angles,<sup>35</sup> was significantly different to that of  $[\text{Ni}^{\text{II}}(\text{S}_2\text{CNET}_2)_2]$  and  $[\text{Ni}^{\text{II}}(\text{S}_2\text{COEt})_2]$  with slightly broader  $L_3$  and  $L_2$  maxima shifted to lower energy at 853.1 and 870.2 eV, respectively. The relative change in energy of the  $L_3$  and  $L_2$  peaks should be noted, and the increase in band width is directly related to the increase in the number of allowed transitions.<sup>5</sup> A shift to lower energy in the  $L_3$  peak on going from square-planar to octahedral geometry for  $\text{Ni}^{\text{II}}$  has been observed but not quantified previously.<sup>11,19</sup> We have identified a shift from 852.8 eV to 853.8 and 854.1 eV on going from tetrahedral  $[\text{NiBr}_2(\text{PPh}_3)_2]$  to *trans*- $[\text{NiBr}_2(\text{PET}_3)_2]$  and *cis*- $[\text{NiBr}_2(\text{dppe})]$  [dppe = 1,2-bis(diphenylphosphino)ethane] square-planar complexes, respectively.<sup>3</sup> Therefore, we believe that the shifts in energy of the  $L_3$  features on changing the geometry at the Ni centre, are primarily related to the changes in energy of the empty (formally antibonding) 3d orbitals, rather than a significant change in the 2p binding energy. The trend (in

terms of energy of the empty 3d orbitals) of tetrahedral < octahedral < square-planar for  $\text{Ni}^{\text{II}}$  is in line with that predicted by ligand field theory and observed by optical spectroscopy.<sup>36</sup> In addition to the changes in the position of the L-edge features, it has been shown<sup>11,12,19,24</sup> both experimentally and theoretically that the branching ratio in  $\text{Ni}^{\text{II}}$  compounds increases on going from a spin paired ( $S = 0$ ) square-planar geometry to a paramagnetic ( $S = 2$ ) tetrahedral or octahedral structure, and that the extent of this is related to the change in the expectation value of the spin–orbit operator in the valence states. Therefore, both the energy position and branching ratios of the  $L_3$  and  $L_2$  features can be used to identify octahedral, tetrahedral and square-planar geometries in  $\text{Ni}^{\text{II}}$  complexes.

In Fig. 1(c), the Ni L-edge spectrum of  $\text{NiS}_2$  is given (this is virtually identical to that published previously,<sup>37</sup> with the  $\text{Ni}^{\text{II}}$  in an octahedral environment with six S atoms at 2.39 Å<sup>38</sup>) and it is clear that there is more structure observed at both the  $L_3$  and  $L_2$  edges in this spectrum than in that of  $[\text{PPh}_4][\text{Ni}^{\text{II}}(\text{S}_2\text{COEt})_3]$ . This difference may be due to either changes in covalency {cf.  $\text{NiBr}_2$  and  $\text{NiI}_2$ ,<sup>10</sup> and  $[\text{Ni}^{\text{II}}(\text{tren})_2][\text{BF}_4]_2$  ( $\text{NiV}_6$ ) [tren = tris-(2-aminoethyl)amine] and  $[\text{Ni}^{\text{II}}(\text{ttcn})_2][\text{BF}_4]_2$  ( $\text{NiS}_6$ ) (ttcn = 1,4,7-trithiacyclononane)<sup>19</sup>} or the presence of a distorted octahedral environment in  $[\text{PPh}_4][\text{Ni}^{\text{II}}(\text{S}_2\text{COEt})_3]$ .<sup>35</sup>

#### Nickel(IV) complexes

For Ni in  $[\text{Ni}^{\text{IV}}(\text{S}_2\text{CNET}_2)_3][\text{BF}_4]$  [Fig. 1(d)], an increase in the formal oxidation state resulted in a shift of the  $L_3$  and  $L_2$  peak maxima to 855.0 eV and 871.7 eV, respectively. There was a weak feature at 859.1 eV together with a pronounced satellite at 861.8 eV. These shifts in the  $L_3$  and  $L_2$  features of ca. 2.0 and 1.4 eV, respectively, on going from octahedral  $\text{Ni}^{\text{II}}$  to octahedral  $\text{Ni}^{\text{IV}}$  are smaller than those predicted by van der Laan<sup>5</sup> (2–4 eV per oxidation state) but are in accord with values obtained for related  $[\text{Ni}(\text{qdt})_2]^-$ <sup>39,40</sup> (qdt = quinoxaline-2,3-dithiolate) and  $[\text{Ni}(\text{pdtc})_2]^-$  (pdtc = pyridine-2,6-dithiocarboxylate) complexes<sup>20</sup> where a shift of ca. 1 eV was observed on going from square-planar  $\text{Ni}^{\text{II}}$  to square-planar (formally)  $\text{Ni}^{\text{III}}$ . We believe that Fig. 1(d) is a representative spectrum of  $[\text{Ni}^{\text{IV}}(\text{S}_2\text{CNET}_2)_3][\text{BF}_4]$  since the same spectral profile was recorded on several different occasions using different preparations of the compound, and in one case where the sample was known to be contaminated with  $\text{Ni}^{\text{II}}$  this was immediately obvious in the spectrum. Although the  $\text{Ni}^{\text{IV}}$  oxidation state is relatively scarce in the realm of molecular compounds, its existence in  $[\text{Ni}^{\text{IV}}(\text{S}_2\text{CN}^n\text{Bu}_2)_3]\text{Br}$  and  $[\text{Ni}^{\text{IV}}(\text{S}_2\text{CNET}_2)_3][\text{C}_3(\text{CN})_3]$  has been shown to be acceptable from a structural standpoint,<sup>41–43</sup> and the value of the magnetic moment ( $\mu_{\text{eff}}$ ) of 0.71  $\mu_{\text{B}}$  for  $[\text{Ni}^{\text{IV}}(\text{S}_2\text{CN}^n\text{Bu}_2)_3]\text{Br}$  was consistent with a low spin  $d^6$  configuration.<sup>42</sup>

#### Effects of prolonged exposure to soft X-rays

Sequential scanning (recorded at the same sample position) of the two square-planar complexes,  $[\text{Ni}^{\text{II}}(\text{S}_2\text{CNET}_2)_2]$  and  $[\text{Ni}^{\text{II}}(\text{S}_2\text{COEt})_2]$ , showed no significant changes in the spectra over several scans. Similarly, the appearance of the first spectra recorded for  $[\text{PPh}_4][\text{Ni}^{\text{II}}(\text{S}_2\text{COEt})_3]$  and  $[\text{Ni}^{\text{IV}}(\text{S}_2\text{CNET}_2)_3][\text{BF}_4]$  [Fig. 1(b) and (d)] were reproducible through several separate runs (over the period of ca. a year) using material from different preparations. However, in contrast to  $[\text{Ni}^{\text{II}}(\text{S}_2\text{CNET}_2)_2]$  and  $[\text{Ni}^{\text{II}}(\text{S}_2\text{COEt})_2]$ , prolonged scans at the same sample position for both  $[\text{PPh}_4][\text{Ni}^{\text{II}}(\text{S}_2\text{COEt})_3]$  and  $[\text{Ni}^{\text{IV}}(\text{S}_2\text{CNET}_2)_3][\text{BF}_4]$  resulted in significant changes in the spectra. Fig. 2 shows successive spectra recorded for  $[\text{PPh}_4][\text{Ni}^{\text{II}}(\text{S}_2\text{COEt})_3]$  over a period of ca. 75 min. It is clear that the  $L_3$  feature moved to slightly higher energy in successive spectra whilst the position of the  $L_2$  peak remained relatively invariant, and that the branching ratio reduced. Whilst the shift of the  $L_3$  peak might be interpreted as the result of an oxidative process, the fact that the  $L_2$  feature remained at a fairly constant value ruled this out. The combin-

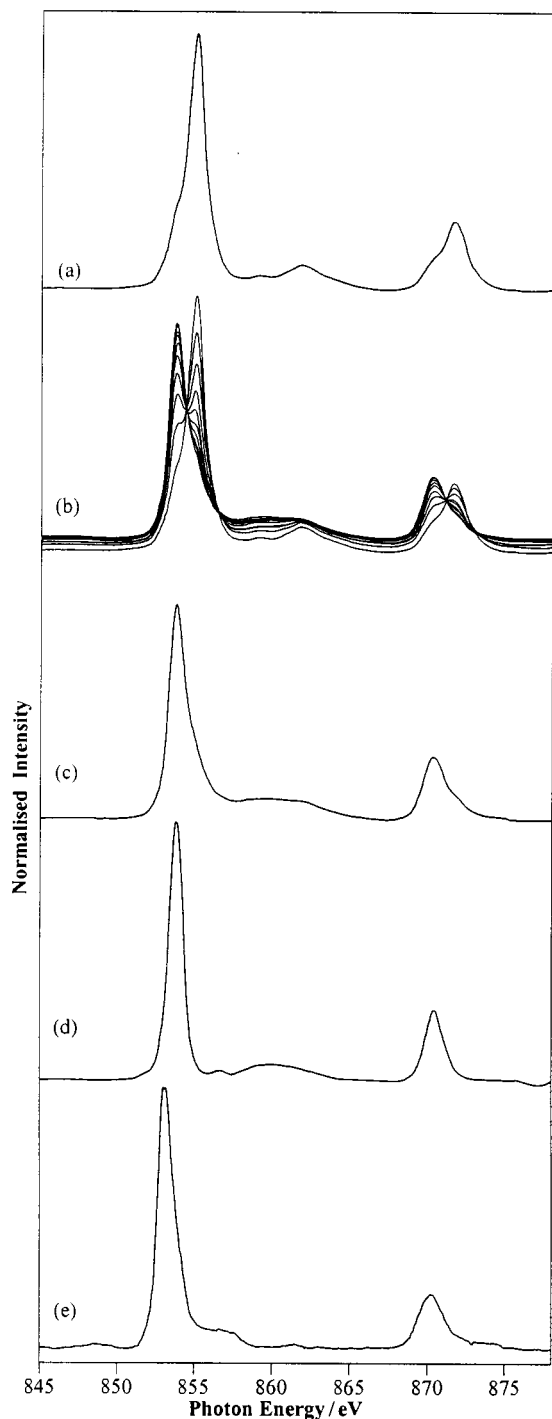


**Fig. 3** Ni L-edge spectra of (a)  $[\text{Ni}^{\text{IV}}(\text{S}_2\text{CNET}_2)_3][\text{BF}_4]$  initial spectrum, (b)  $[\text{Ni}^{\text{IV}}(\text{S}_2\text{CNET}_2)_3][\text{BF}_4]$  successive spectra, (c)  $[\text{Ni}^{\text{IV}}(\text{S}_2\text{CNET}_2)_3][\text{BF}_4]$  final spectrum, (d)  $[\text{Ni}^{\text{II}}(\text{S}_2\text{CNET}_2)_2]$ , and (e)  $[\text{PPh}_4][\text{Ni}^{\text{II}}(\text{S}_2\text{COEt})_3]$ .

ation of the shifts in the  $L_{2,3}$  peaks and the change in the branching ratio are taken to indicate that when  $[\text{PPh}_4][\text{Ni}^{\text{II}}(\text{S}_2\text{COEt})_3]$  is exposed to soft X-rays, it is changed photochemically from a  $\text{Ni}^{\text{II}}$  octahedral complex into a  $\text{Ni}^{\text{II}}$  species that is almost certainly square planar. This interpretation was confirmed by comparison of the final spectrum with that of square planar  $[\text{Ni}^{\text{II}}(\text{S}_2\text{COEt})_2]$  shown in Fig. 2(d).

Fig. 3 shows the effect of soft X-ray irradiation on the spectra of  $[\text{Ni}^{\text{IV}}(\text{S}_2\text{CNET}_2)_3][\text{BF}_4]$ . Fig. 3(a) shows the initial spectrum, Fig. 3(b) the effect of soft X-ray irradiation and Fig. 3(c) the final spectrum after ca. 170 min. In contrast to the irradiation of  $[\text{PPh}_4][\text{Ni}^{\text{II}}(\text{S}_2\text{COEt})_3]$ , both the  $L_3$  and  $L_2$  features moved to lower energy in successive spectra. The appearance of the final spectrum of  $[\text{Ni}^{\text{IV}}(\text{S}_2\text{CNET}_2)_3][\text{BF}_4]$  [Fig. 3(c)] with  $L_3$  and  $L_2$  maxima at 853.8 and 870.3 eV, respectively,

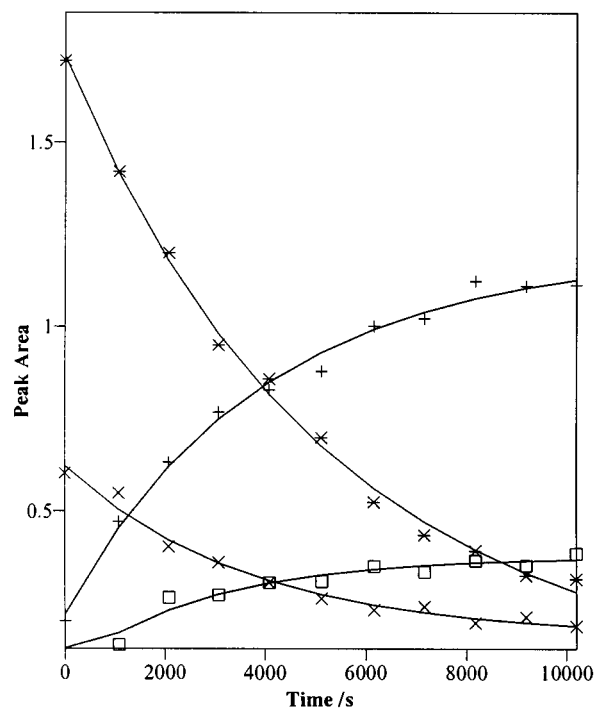


**Fig. 4** Plots showing the decay and growth of peaks in the Ni L-edge spectra of  $[\text{Ni}^{\text{IV}}(\text{S}_2\text{CNET}_2)_3][\text{BF}_4]$ . Solid lines represent best fit exponential curves. 853.8 eV (+) ( $A_0 = 0.22(3)$ ,  $A_\infty = 1.21(4)$ ,  $k = 2.5(3) \times 10^{-4} \text{ s}^{-1}$ ,  $R^2 = 0.992$ ); 855.0 eV (\*) ( $A_0 = 1.73(3)$ ,  $A_\infty = 0.03(6)$ ,  $k = 1.9(2) \times 10^{-4} \text{ s}^{-1}$ ,  $R^2 = 0.996$ ); 870.3 eV (□) ( $A_0 = 0.07(2)$ ,  $A_\infty = 0.38(2)$ ,  $k = 3.5(6) \times 10^{-4} \text{ s}^{-1}$ ,  $R^2 = 0.963$ ); 871.7 eV (×) ( $A_0 = 0.62(2)$ ,  $A_\infty = 0.16(2)$ ,  $k = 2.7(4) \times 10^{-4} \text{ s}^{-1}$ ,  $R^2 = 0.981$ ). ( $A_0$  = calculated initial peak area,  $A_\infty$  = calculated peak area at  $t = \infty$ ,  $k$  = first order rate constant,  $R^2$  = fit parameter.)

was remarkably similar to that of  $[\text{Ni}^{\text{II}}(\text{S}_2\text{CNET}_2)_2]$  [Fig. 3(d)] with  $L_3$  and  $L_2$  maxima at 853.8 and 870.4 eV, whilst in the spectrum of  $[\text{PPh}_4][\text{Ni}^{\text{II}}(\text{S}_2\text{COEt})_3]$  [Fig. 3(e)], the  $L_3$  and  $L_2$  features were at 853.1 and 870.2 eV, respectively. Therefore, we believe that on exposure to soft X-rays  $[\text{Ni}^{\text{IV}}(\text{S}_2\text{CNET}_2)_3][\text{BF}_4]$  is photoreduced from a six co-ordinate octahedral  $\text{Ni}^{\text{IV}}$  complex to a four co-ordinate square-planar  $\text{Ni}^{\text{II}}$  compound, a process we describe as soft X-ray photoreduction (SOXPR). To ensure that these effects could not simply be related to sample stability, comparisons were made between freshly prepared samples and the original (aged) batches of  $[\text{Ni}^{\text{II}}(\text{S}_2\text{CNET}_2)_2]$  and  $[\text{Ni}^{\text{IV}}(\text{S}_2\text{CNET}_2)_3][\text{BF}_4]$ , with no differences related to the age of the sample being observed.

#### Factors affecting rate of photochemistry

The reproducibility of both the spectra and soft X-ray photochemical processes occurring in  $[\text{PPh}_4][\text{Ni}^{\text{II}}(\text{S}_2\text{COEt})_3]$  and  $[\text{Ni}^{\text{IV}}(\text{S}_2\text{CNET}_2)_3][\text{BF}_4]$  at the Ni L-edge prompted further investigation, especially as reports of radiation damage or other changes observed during 3d L-edge XAFS experiments are very sparse. In addition, spectra recorded of the same samples at the Ni K-edge<sup>44</sup> appeared unchanged after multiple scans. As the spectral changes were more marked in  $[\text{Ni}^{\text{IV}}(\text{S}_2\text{CNET}_2)_3][\text{BF}_4]$  than in  $[\text{PPh}_4][\text{Ni}^{\text{II}}(\text{S}_2\text{COEt})_3]$ , the former was chosen for the more detailed study which used the experimental protocol outlined earlier to allow for comparison between spectra collected at different times.

The presence of the well defined isosbestic points at 854.4 and 871.1 eV in the successive spectra of  $[\text{Ni}^{\text{IV}}(\text{S}_2\text{CNET}_2)_3][\text{BF}_4]$  [Fig. 3(b)] clearly suggested that a 'state-to-state transformation' was occurring, rather than sample degradation. The change in areas of the peaks centred on 853.8, 855.0, 870.3 and 871.7 eV (which correspond to the  $\text{Ni}^{\text{II}}$   $L_3$ -edge,  $\text{Ni}^{\text{IV}}$   $L_3$ -edge,  $\text{Ni}^{\text{II}}$   $L_2$ -edge and  $\text{Ni}^{\text{IV}}$   $L_2$ -edge features, respectively) are shown

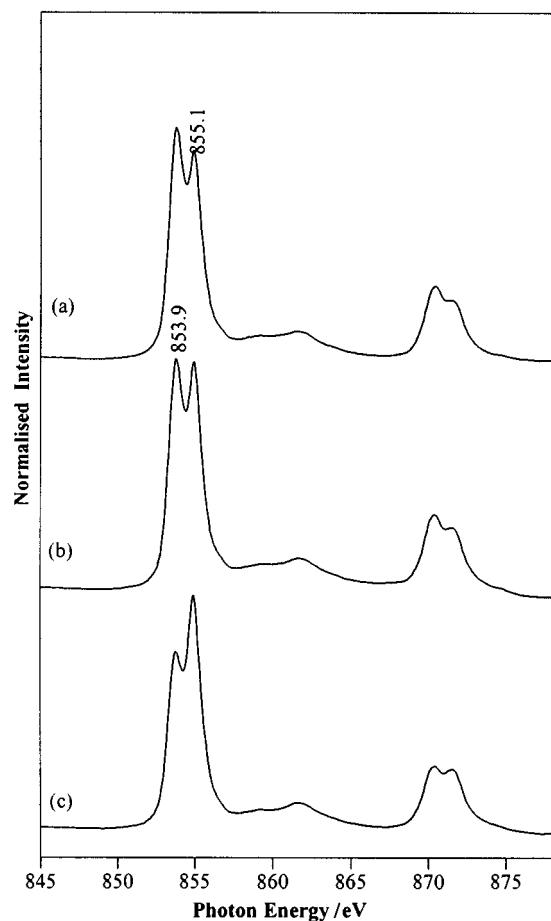


Fig. 5 Ni L-edge spectra of  $[\text{Ni}^{\text{IV}}(\text{S}_2\text{CNET}_2)_3][\text{BF}_4]$  recorded after exposure to (a) 855.1 eV, (b) 853.9 eV and (c) 842.7 eV for 20 min.

in Fig. 4, together with best fit exponential decay curves. The areas of the  $\text{Ni}^{\text{IV}}$  peaks were greater than those of the  $\text{Ni}^{\text{II}}$  peaks at both the  $\text{L}_3$  and  $\text{L}_2$  edges, as to be expected from the change in the number of electron-holes.<sup>23b</sup> The first-order rate constants,  $k$ , were  $\text{ca. } 2 \times 10^{-4} \text{ s}^{-1}$  for all four curves indicating that the decay of the  $\text{Ni}^{\text{IV}}$  species and the appearance of the  $\text{Ni}^{\text{II}}$  species obeyed the same kinetics, and therefore, are intimately linked. The first order rate constants determined from solution NMR measurements during optical photochemistry (Hg–Xe 1000 W lamp  $\lambda > 325 \text{ nm}$ ) of  $[\text{Ni}^{\text{IV}}(\text{S}_2\text{CN}(\text{CH}_2\text{Ph})_2)_3]\text{Br}$  were of the order  $2 \times 10^{-4}$  to  $4.5 \times 10^{-3} \text{ s}^{-1}$  depending on the lamp intensity.<sup>45</sup> The quantum yields observed in the solution NMR studies were of the order of 0.1–0.2,<sup>45</sup> whilst we have not been able to carry out experiments in sufficient detail to determine the soft X-ray quantum yields, approximate, semi-quantitative calculations, based on molecular volumes, penetration depths and photon flux, indicated that the soft X-ray quantum yields were also of the order of about 0.1.

The effect of the incident X-ray energy was examined because irradiation at the Ni L-edge ( $\text{ca. } 855 \text{ eV}$ ) but not at the Ni K-edge ( $\text{ca. } 8335 \text{ eV}$ )<sup>44</sup> had resulted in photochemical transformation in the  $\text{Ni}^{\text{IV}}$  samples. The Ni L-edge spectra recorded after irradiation at  $\text{ca. } 120$ ,  $\text{ca. } 165 \text{ eV}$  and after scanning through the S L-edge ( $\text{ca. } 120\text{--}180 \text{ eV}$ ) were all similar, and showed a lesser rate of change than that observed for spectra acquired for the same length of time at the Ni L-edge. This indicated that, although some change occurred with low energy soft X-ray irradiation, the rate of decay was slower than irradiation at the Ni L-edge. A set of resonance experiments both on and off the Ni L-edge was also undertaken (Fig. 5). Comparison of the spectra recorded after irradiation at 855.1 [Fig. 5(a)], 853.9 [Fig. 5(b)] and 842.7 eV [Fig. 5(c)], corresponding to irradiation for 20 minutes at the  $\text{Ni}^{\text{IV}}$   $\text{L}_3$ -edge, at the  $\text{Ni}^{\text{II}}$   $\text{L}_3$ -

edge and before the Ni L-edges, respectively, revealed an apparently strong resonance effect. It is clear that there was a much greater rate of change when the sample was irradiated into the  $\text{Ni}^{\text{IV}}$   $\text{L}_3$  absorption bands rather than in the pre-edge region, and that this accelerated rate of change was also greater for irradiation into the  $\text{Ni}^{\text{IV}}$   $\text{L}_3$  band compared with the  $\text{Ni}^{\text{II}}$   $\text{L}_3$  band, indicating that the rate of photoreduction was photon energy dependent. These results indicate that the photoreduction may be largely a metal-based rather than a ligand-based phenomenon.<sup>46</sup>

To investigate the effect of temperature, a sample of  $[\text{Ni}^{\text{IV}}(\text{S}_2\text{CNET}_2)_3][\text{BF}_4]$  was cooled to  $\text{ca. } 55 \text{ K}$  and sequential spectra, using a previously non-irradiated sample position, were recorded. In comparison to the decay profile observed at room temperature, the rate of decay at 55 K was practically unchanged, indicating that in this case the rate of photoreduction was largely temperature independent. In the previous laser flash photolysis study of  $[\text{Ni}^{\text{IV}}(\text{S}_2\text{CN}^n\text{Bu})_3]\text{Br}$ , the quantum yield was found to be temperature independent (300–240 K), but the lifetime of the excited state increased from 25 ns to 1  $\mu\text{s}$  on reducing the temperature. This was interpreted to imply that the photochemical processes were occurring in an excited triplet state rather than in a singlet state.<sup>47,48</sup>

To assess the effect of photon flux, spectra of  $[\text{Ni}^{\text{IV}}(\text{S}_2\text{CNET}_2)_3][\text{BF}_4]$  were recorded just before and directly after a fresh electron beam was introduced into the storage ring. This was the only practical means of reducing the total flux whilst maintaining the same spot size and resolution, as both of these would be affected by a change in the position of the exit slits. The difference in beam current, which is directly related to photon flux, was approximately 100 mA (150 *cf.* 250 mA) which made a difference of about 5/3 in the photon flux delivered to the sample. Under these conditions, the rate of decay observed with higher beam currents in a new beam was substantially greater than that with an 'old' beam. In one particular experiment, three scans with the new beam were required to achieve the same extent of change in the spectrum that required four scans just prior to beam refill. Similar behaviour has been observed during visible light photolysis of  $[\text{Ni}^{\text{IV}}(\text{S}_2\text{CN}(\text{CH}_2\text{Ph})_2)_3]\text{Br}$  monitored by solution NMR where an approximately linear relationship between relative light intensity and first order rate constant was observed.<sup>45</sup> Therefore, the rate of soft X-ray induced photoreduction was photon flux dependent.

Although the above results relate to  $[\text{Ni}^{\text{IV}}(\text{S}_2\text{CNET}_2)_3][\text{BF}_4]$ , further experiments using  $[\text{Ni}^{\text{IV}}(\text{S}_2\text{CN}^n\text{Bu})_3][\text{BF}_4]$  were also carried out to check the effect of the ligands on the rate of photoreduction. The rate of decay observed for  $[\text{Ni}^{\text{IV}}(\text{S}_2\text{CN}^n\text{Bu}_2)_3][\text{BF}_4]$  was significantly greater (2–3 fold) than that for  $[\text{Ni}^{\text{IV}}(\text{S}_2\text{CNET}_2)_3][\text{BF}_4]$ . The different electron donating properties of Et and  $^n\text{Bu}$  groups in  $[\text{Ni}(\text{S}_2\text{CNET}_2)_2]$  and  $[\text{Ni}(\text{S}_2\text{CN}^n\text{Bu}_2)_2]$  have been investigated using XPS and Auger spectroscopies.<sup>49</sup> The Ni 2p<sub>3/2</sub>, S 2p and N 1s XPS binding energies were found to increase by 0.46, 0.53 and 0.44 eV, respectively, on going from  $[\text{Ni}(\text{S}_2\text{CNET}_2)_2]$  to  $[\text{Ni}(\text{S}_2\text{CN}^n\text{Bu}_2)_2]$ , and these trends were also reflected in the Auger spectra. These observations were interpreted as indicating that  $[\text{S}_2\text{CNET}_2]^-$  was a better electron donor ligand than  $[\text{S}_2\text{CN}^n\text{Bu}_2]^-$ .<sup>49,50</sup> Such behaviour if found in the  $\text{Ni}^{\text{IV}}$  complexes would lead to the  $^n\text{Bu}$  groups making reduction to  $\text{Ni}^{\text{II}}$  more facile as compared to Et groups. Also, it is likely that the different rates of photoreduction are related to subtle differences in solid state packing effects and the ease of structural reorganisation, which may have an important bearing on the structural changes associated with the photochemical transformations, as discussed below.

To compare the effect of soft X-ray and visible irradiation<sup>42,47,48,51</sup> of the sample, the Al foil and plastic cover from one of the UHV sample chamber viewports were removed and a fresh sample of  $[\text{Ni}^{\text{IV}}(\text{S}_2\text{CNET}_2)_3][\text{BF}_4]$  was irradiated with visible light (400–700 nm) for 15 minutes in the absence of soft

X-rays. The Ni L-edge spectrum recorded after this visible irradiation showed a greater rate of change due to the visible light as compared with that induced by soft X-ray irradiation, but with the same form of decay profile being recorded during the successive Ni L-edge spectra. The similarity of the Ni L-edge spectra obtained after both soft X-ray or visible irradiation of  $[\text{Ni}^{\text{IV}}(\text{S}_2\text{CNET}_2)_3][\text{BF}_4]$  indicates that similar processes are probably at work in both cases, and implies that the same overall photochemistry may be occurring in the solid state with soft X-ray irradiation as with visible light.<sup>47</sup> A previously soft X-ray irradiated sample of  $[\text{Ni}^{\text{IV}}(\text{S}_2\text{CNET}_2)_3][\text{BF}_4]$  showing a considerable extent of photoreduction was left in the dark (both visible and soft X-ray) for *ca.* 1 h. Subsequent scanning over the Ni L-edge at the same sample position showed no detectable reversion to the  $\text{Ni}^{\text{IV}}$  state, implying the absence of the so-called 'dark reaction' previously observed when the dark colour of the  $\text{Ni}^{\text{IV}}$  species returned to give a product spectroscopically identical to the starting material when the acetonitrile, ethanol and methanol solutions<sup>47,48</sup> and solid PMMA matrices<sup>48</sup> were left in the dark. However, it should be noted that no such 'dark reaction' was reported when frozen methanol matrices were used.<sup>47</sup>

## Discussion

Reports of radiation-induced chemical damage or photochemistry occurring during 3d  $L_{2,3}$ -edge experiments are sparse in the literature although such behaviour might be expected by comparison to the radiation damage observed in XPS studies.<sup>52–55</sup> Comments in the literature with respect to 3d L-edge work and radiation damage are generally restricted to statements such as: 'To minimise radiation damage, the position of the X-ray beam on the sample was moved every few scans. No evidence was observed for changes over time in the beam'<sup>20</sup> and 'the experiments were carried out at low temperature, and that no significant changes in absorption spectra . . . were observed in the temperature range 10–293 K.'<sup>56</sup> However, some photoreduction, in a  $\text{Mn}^{\text{IV}}$  catalase has been observed, but not in the associated model compounds.<sup>57</sup> Of particular relevance to this work, no radiation damage or photochemical changes were reported for a range of molecular  $\text{Ni}^{\text{II}}$  and  $\text{Ni}^{\text{III}}$  complexes as well as Ni-containing proteins,<sup>19,20</sup> although it should be pointed out that the experiments were conducted at *ca.* 10 K.

Generally, examples of sample decomposition occurring during XPS experiments have involved compounds of transition elements, where a chemical shift of a metal-core level can be correlated with a reduction in valence of the metal ion,<sup>54,55</sup> and the oxidation state of the decomposition product usually corresponds to that expected from simple chemical experience. For example, there have been mechanistic studies on the rates of photoreduction of  $\text{Fe}^{\text{III}}$  in  $[\text{K}_3\{(\text{Fe},\text{Co})(\text{CN})_6\}]$ <sup>58</sup> and  $\text{Pt}^{\text{IV}}$  in  $[\text{Pt}^{\text{IV}}(\text{en})\text{Cl}_4]$ ,  $[\text{Pt}^{\text{II}}(\text{en})\text{Cl}_2 \cdot \text{Pt}^{\text{IV}}(\text{en})\text{Cl}_4]$ ,  $[\text{Pt}^{\text{IV}}(\text{en})_2\text{Cl}_2]\text{Cl}_2$ ,  $\text{K}_2[\text{Pt}^{\text{IV}}\text{Cl}_4]$  and  $\text{K}_2[\text{Pt}^{\text{IV}}(\text{CN})_4\text{Cl}_2]$ .<sup>59</sup> However, of direct relevance to our work, are XPS studies of metal dithiocarbamate complexes which have a tendency to give inconsistent results, a feature taken to mean chemical instability under XPS conditions. Also, it was noted that Cu complexes containing Cu–S linkages exhibited significantly greater photoreduction than those with N and/or O bonds to the metal.<sup>60</sup> In particular, an XPS study of a series of  $\text{Cu}^{\text{II}}$  complexes containing N,N'-cyclic substituted dithiocarbamates resulted in spectra that were interpreted as resulting from reduction to  $\text{Cu}^{\text{I}}$  after irradiation of >1 h.<sup>61</sup> It is significant that no spectral changes were reported for a series of cobalt(II) dtc complexes.<sup>62</sup>

In the case of  $[\text{Ni}^{\text{IV}}(\text{S}_2\text{CNET}_2)_3][\text{BF}_4]$  we have shown that the rate of decay is dependent on photon flux, photon energy and ligand, but is largely independent of temperature. Therefore, from comparison with XPS data, it would appear that SOXPC resulting in photoreduction would be expected to be observed

more frequently than it has to date. For example, in the case of  $\text{K}_3[\text{Fe}(\text{CN})_6]$  we have observed<sup>63</sup> significant photoreduction at 300 K to a species whose Fe L-edge spectrum is very similar to that of  $\text{K}_4[\text{Fe}(\text{CN})_6]$  whilst at 50 K the rate of change was considerably reduced, but neither of these observations were reported in the previous Fe L-edge study.<sup>64</sup> We have also observed photoreduction in  $[\text{Co}(\text{acac})_3]$  and  $[\text{Cp}_2\text{Fe}][\text{BF}_4]$ <sup>65</sup> as well as in some vanadium complexes.<sup>2</sup>

One possible explanation for the lack of photochemistry observed in the previous L-edge studies, is that our experiments have been carried out using an undulator beamline with focusing optics, which delivers a considerably larger photon flux to the sample compared to a bending magnet beamline. This obviously has very severe consequences and implications for carrying out 3d L-edge experiments on third generation synchrotron sources where the photon flux will be even higher.

Whilst there is a well developed photochemistry of dithiocarbamate complexes (iron, nickel, molybdenum and ruthenium complexes have recently been reviewed<sup>65</sup>), that for xanthate complexes is very sparse.  $[\text{Ni}^{\text{IV}}(\text{S}_2\text{CN}^n\text{Bu}_2)_3]\text{Br}$  was the first reported<sup>41</sup> nickel-dtc complex to be optically photoactive, and the optical photochemistry of this and related  $\text{Ni}^{\text{IV}}$  dtc complexes have been investigated using UV/VIS<sup>41,42</sup> and NMR<sup>45</sup> spectroscopies, and more recently, both in solution and in the solid state, using a combination of electronic absorption spectroscopy and laser flash photolysis.<sup>47,48</sup> In solution,  $[\text{Ni}^{\text{IV}}(\text{S}_2\text{CNR}_2)_3]\text{Br}$  ( $\text{R} = n\text{Bu}$ ,<sup>42,47,48</sup>  $\text{CH}_2\text{Ph}$ <sup>45</sup>) have been shown to be photoreduced to  $[\text{Ni}^{\text{II}}(\text{S}_2\text{CNR}_2)_2]$ ,  $\text{NiBr}_2$  and the corresponding thiuramdisulfide (tds), with a dark reaction resulting in the re-formation of  $[\text{Ni}^{\text{IV}}(\text{S}_2\text{CNR}_2)_3]\text{Br}$ . Of more relevance to our studies are experiments carried out in frozen methanol matrices at 77 K where the quantum yields were reduced by three orders of magnitude. After a detailed investigation of the changes occurring in the electronic absorption spectra, the photochemical changes were rationalised on the basis of the homolytic cleavage of two Ni–S bonds with the overall reduction of  $\text{Ni}^{\text{IV}}$  to  $\text{Ni}^{\text{II}}$  and oxidation of two dtc moieties to form a thiuramdisulfide (tds) ligand.<sup>47</sup>

As the Ni L-edge spectra of  $[\text{Ni}^{\text{IV}}(\text{S}_2\text{CNET}_2)_3][\text{BF}_4]$  have the same form after both visible and soft X-ray photochemistry, it is reasonable to assume that the same kind of process could be occurring in both cases, even though the visible photochemistry results from a ligand to metal charge transfer transition whereas the soft X-ray photochemistry arises from  $2p \rightarrow 3d$  transitions and photoionisation. Although the optical photochemical pathway involving homolytic cleavage of Ni–S bonds can be used to account for soft X-ray photoreduction in  $[\text{Ni}^{\text{IV}}(\text{S}_2\text{CNET}_2)_3][\text{BF}_4]$ , unfortunately, consideration of the electron balance shows that this does not account for the change from octahedral  $\text{Ni}^{\text{IV}}$  to square-planar  $\text{Ni}^{\text{II}}$  in  $[\text{PPh}_4][\text{Ni}^{\text{II}}(\text{S}_2\text{COEt})_3]$ . An alternative explanation is that instead of the homolytic cleavage of the Ni–S bonds it is possible that the absorption of soft X-ray photons, to give the excited state configuration of  $2p^5 3d^9$ , results in the transformation of two of the bidentate xan ligands into monodentate ligands and this would maintain both the metal oxidation state and the overall charge of the complex. It is conceivable that this sort of process could also be occurring in the photo-reduction of  $[\text{Ni}^{\text{IV}}(\text{S}_2\text{CNET}_2)_3][\text{BF}_4]$ , with either the formation of a tris-dtc  $\text{Ni}^{\text{II}}$  complex, which then re-organises to a square-planar geometry, or the formation of a  $\text{Ni}^{\text{IV}}$  square-planar centre that is then photoreduced. Of these, the first is the more likely, as it is known that tris-dtc  $\text{Ni}^{\text{II}}$  complexes are very unstable, with the formation constant,  $K_3$ , for the tris-dtc  $\text{Ni}^{\text{II}}$  complex being about three orders of magnitude less than that for the corresponding xanthate complex.<sup>35</sup> Unfortunately, from our data it is not possible to identify which mechanism best accounts for the soft X-ray photochemical processes occurring in  $[\text{Ni}^{\text{IV}}(\text{S}_2\text{CNET}_2)_3][\text{BF}_4]$  and  $[\text{PPh}_4][\text{Ni}^{\text{II}}(\text{S}_2\text{COEt})_3]$ , and as the L-edge experiments are surface sensitive (*ca.* 30–50 Å) there is also no easy way to be able to differentiate

between the two competing mechanisms using other spectroscopic techniques.

## Conclusions

The sensitivity of  $L_{2,3}$ -edge XAFS to oxidation state and local environment has allowed us to demonstrate that soft X-ray radiation is capable of producing photoreduction of the metal and/or a change in co-ordination number in Ni-S chelate complexes. We have shown that when  $[\text{Ni}^{\text{IV}}(\text{S}_2\text{CNET}_2)_3][\text{BF}_4]$  is exposed to soft X-rays there is a reduction in both co-ordination number and oxidation state of the metal, consistent with the formation of a square-planar  $\text{Ni}^{\text{II}}$  centre. The rate of photochemical transformation for  $[\text{Ni}^{\text{IV}}(\text{S}_2\text{CNR}_2)_3][\text{BF}_4]$  is proportional to the photon flux and is also dependent on the ligands bonded to the nickel centre, but is virtually independent of temperature. The results of our experiments show a strong resonance effect, with irradiation into the Ni L-edge absorption band of the photoactive species producing the greatest effect, and the products of this soft X-ray photochemistry may be related to those expected from conventional chemistry. Also, we have shown that when  $[\text{PPh}_4][\text{Ni}^{\text{II}}(\text{S}_2\text{COEt})_3]$  is exposed to soft X-rays it is converted from a six co-ordinate octahedral complex into a square-planar  $\text{Ni}^{\text{II}}$  complex.

Whilst the soft X-ray photochemical transformation of formally  $\text{Ni}^{\text{IV}}$  complexes may be expected, we have also observed significant soft X-ray induced effects in a wide range of complexes.<sup>1,2,63</sup> Therefore, we believe that soft X-ray induced photochemical changes may be more prevalent and pernicious in 3d L-edge work than previously thought, and caution dictates that such processes should be assumed to be possible or probable in a large number of other systems. We recommend that when recording soft X-ray absorption spectra, checks are made either to identify or to rule out photochemical reactions by the recording of successive spectra at the same sample position, utilising a simultaneous *in situ* calibration system. These observations have a serious consequence on the use of 3d L-edge XAFS at third generation synchrotron sources.

## Acknowledgements

We gratefully acknowledge: the EPSRC/SERC for an Advanced Fellowship (N. A. Y.), equipment and SRS beamtime (GR/J 34200), personnel (C. M. McG., GR/K 64662) a post-graduate studentship (J. M. W. S.) and access to the Chemical Database Service at Daresbury;<sup>66</sup> The Royal Society for a University Research Fellowship (D. C.); The University of Manchester for a Rona Robinson Scholarship (E. P.), The University of Hull and The University of Manchester for equipment; and the Director of the Synchrotron Radiation Division at Daresbury Laboratory for access to synchrotron and computing facilities.

## References

- 1 Part 1. D. Collison, C. D. Garner, C. M. McGrath, J. F. W. Mosselmans, M. D. Roper, J. M. W. Seddon, E. Sinn and N. A. Young, *J. Chem. Soc., Dalton Trans.*, 1997, 4371.
- 2 D. Collison, C. D. Garner, J. Grigg, C. M. McGrath, J. F. W. Mosselmans, E. Pidcock, M. D. Roper, J. M. W. Seddon, E. Sinn, P. A. Tasker, G. Thornton, J. F. Walsh and N. A. Young, *J. Chem. Soc., Dalton Trans.*, 1998, 2199.
- 3 M. J. Ashcroft, D. Collison, C. D. Garner, J. F. W. Mosselmans, E. Pidcock and N. A. Young, *Physica B*, 1995, **208–209**, 725.
- 4 M. Medarde, A. Fontaine, J. L. García-Muñoz, J. Rodríguez-Carvajal, M. de Santis, M. Sacchi, G. Rossi and P. Lacorre, *Phys. Rev. B*, 1992, **46**, 14975.
- 5 G. van der Laan and I. W. Kirkman, *J. Phys.: Condens. Matter*, 1992, **4**, 4189.
- 6 M. O. Krause and J. H. Oliver, *J. Phys. Chem. Ref. Data*, 1979, **8**, 329.
- 7 See ref. 1, and references therein.
- 8 F. M. F. de Groot, *J. Electron Spectrosc. Relat. Phenom.*, 1994, **67**, 529.

- 9 E. E. Koch, Y. Jugnet and F. J. Himpsel, *Chem. Phys. Lett.*, 1985, **116**, 7.
- 10 G. van der Laan, J. Zaanen, G. A. Sawatzky, R. Karnatak and J.-M. Esteve, *Phys. Rev. B*, 1986, **33**, 4253.
- 11 G. van der Laan, B. T. Thole, G. A. Sawatzky and M. Verdaguer, *Phys. Rev. B*, 1988, **37**, 6587.
- 12 G. van der Laan and B. T. Thole, *Phys. Rev. Lett.*, 1988, **60**, 1977.
- 13 J. van Elp, B. G. Searle, G. A. Sawatzky and M. Sacchi, *Solid State Commun.*, 1991, **80**, 67.
- 14 M. A. van Veenendaal and G. A. Sawatzky, *Phys. Rev. B*, 1994, **50**, 11326.
- 15 G. Meitzner, D. A. Fischer and J. H. Sinfelt, *Catal. Lett.*, 1992, **15**, 219.
- 16 T. Mizokawa, A. Fujimori, T. Arima, Y. Tokura, N. Mori and J. Akimitsu, *Phys. Rev. B*, 1995, **52**, 13865.
- 17 M. Nakamura, A. Fujimori, M. Sacchi, J. C. Fuggle, A. Misu, T. Momori, H. Tamura, M. Matoba and S. Anzai, *Phys. Rev. B*, 1993, **48**, 16942.
- 18 M. A. van Veenendaal, D. Alders and G. A. Sawatzky, *Phys. Rev. B*, 1995, **51**, 13966.
- 19 J. van Elp, G. Peng, B. G. Searle, S. Mitra-Kirtley, Y.-H. Huang, M. K. Johnson, Z. H. Zhou, M. W. W. Adams, M. J. Maroney and S. P. Cramer, *J. Am. Chem. Soc.*, 1994, **116**, 1918.
- 20 J. van Elp, G. Peng, Z. H. Zhou, M. W. W. Adams, N. Baidya, P. K. Mascharak and S. P. Cramer, *Inorg. Chem.*, 1995, **34**, 2501.
- 21 D. Alders, T. Hibma, G. A. Sawatzky, K. C. Cheung, G. E. van Dorssen, M. D. Roper, H. A. Padmore, G. van der Laan, J. Vogel and M. Sacchi, *J. Appl. Phys.*, 1997, **82**, 3120.
- 22 P. Kuiper, J. van Elp, D. E. Rice, D. J. Buttrey, H. J. Lin and C. T. Chen, *Phys. Rev. B*, 1998, **57**, 1552.
- 23 (a) T. Hatsui, Y. Takata, N. Kosugi, K. Yamamoto, T. Yokoyama and T. Ohta, *J. Electron Spectrosc. Relat. Phenom.*, 1998, **88–91**, 405; N. Kosugi, *J. Electron Spectrosc. Relat. Phenom.*, 1998, **92**, 151; T. Hatsui, Y. Takata and N. Kosugi, *Chem. Phys. Lett.*, 1998, **284**, 320; (b) H. Wang, P. Ge, C. G. Riordan, S. Brooker, C. G. Woerner, T. Collins, C. A. Melendres, O. Graudejus, N. Bartlett and S. P. Cramer, *J. Phys. Chem. B*, 1998, **102**, 8343.
- 24 B. T. Thole and G. van der Laan, *Phys. Rev. B*, 1988, **38**, 3158.
- 25 P. Gütllich and A. Hauser, *Coord. Chem. Rev.*, 1990, **97**, 1; P. Gütllich, A. Hauser and H. Spiering, *Angew. Chem., Int. Ed. Engl.*, 1994, **33**, 2024.
- 26 P. Gütllich, J. Ensling and F. Tuczek, *Hyperfine Int.*, 1994, **84**, 447; P. Gütllich and J. Jung, *Nuovo Cimento. Della Soc. Ital. Fis. D*, 1996, **18**, 107; P. Gütllich, *Mol. Cryst. Liq. Cryst. A*, 1997, **305**, 17.
- 27 H. J. Cavell and S. Sugden, *J. Chem. Soc.*, 1935, 621.
- 28 A. R. Hendrickson, R. L. Martin and N. M. Rohde, *Inorg. Chem.*, 1975, **14**, 2980.
- 29 G. W. Watt and B. J. McCormick, *J. Inorg. Nucl. Chem.*, 1965, **27**, 898.
- 30 By adaptation of the procedure used to prepare  $[\text{NMe}_3\text{Ph}][\text{Ni}(\text{S}_2\text{COEt})_3]$ , D. Coucouvanis and J. P. Fackler Jr., *Inorg. Chem.*, 1967, **6**, 2047.
- 31 C. S. Mythen, G. van der Laan and H. A. Padmore, *Rev. Sci. Instrum.*, 1992, **63**, 1313.
- 32 E. J. Billo, *Excel for Chemists, A Comprehensive Guide*, Wiley-VCH, New York, 1997.
- 33 R. Selvaraju, K. Panchanatheswaran, A. Thiruvalluvar and V. Parthasarathi, *Acta Crystallogr., Sect. C*, 1995, **51**, 606.
- 34 J. P. Crocombette and F. Jollet, *J. Phys.: Condens. Matter*, 1996, **8**, 5253.
- 35 S. B. Choudhury, D. Ray and A. Chakravorty, *Inorg. Chem.*, 1990, **29**, 4603.
- 36 A. B. P. Lever, *Inorganic Electronic Spectroscopy*, Elsevier, Amsterdam, 2nd edn., 1984.
- 37 J. M. Charnock, C. M. B. Henderson, J. F. W. Mosselmans and R. A. D. Patrick, *Phys. Chem. Miner.*, 1996, **23**, 403.
- 38 E. Nowack, D. Schwarzenbach and T. Hahn, *Acta Crystallogr., Sect. B*, 1991, **47**, 650.
- 39 M. J. Ashcroft, Ph.D. Thesis, The University of Manchester, 1994.
- 40 E. Pidcock, Ph.D. Thesis, The University of Manchester, 1995.
- 41 A. Avdeef, J. P. Fackler Jr. and R. G. Fischer Jr., *J. Am. Chem. Soc.*, 1970, **92**, 6972.
- 42 J. P. Fackler Jr., A. Avdeef and R. G. Fischer Jr., *J. Am. Chem. Soc.*, 1973, **95**, 774.
- 43 W. Chen, H. Li, Z.-J. Zhong, K.-L. Zhang and X.-Z. You, *Acta Crystallogr., Sect. C*, 1996, **52**, 3030.
- 44 C. M. McGrath, J. M. W. Seddon, E. Sinn and N. A. Young, unpublished observations.
- 45 D. P. Schwendiman and J. I. Zink, *J. Am. Chem. Soc.*, 1976, **98**, 1248.
- 46 K. B. Pandeya, T. S. Waraich, R. C. Gaur and R. P. Singh, *J. Inorg. Nucl. Chem.*, 1981, **43**, 3159.

- 47 V. F. Plyusnin, V. P. Grivin, N. M. Bazhin, E. P. Kuznetzova and S. V. Larionov, *J. Photochem., Photobiol. A*, 1993, **74**, 121.
- 48 V. F. Plyusnin, V. P. Grivin, N. M. Bazhin, E. P. Kuznetzova and S. V. Larionov, *J. Photochem., Photobiol. A*, 1993, **74**, 129.
- 49 R. Payne, R. J. Magee and J. Liesegang, *J. Electron Spectrosc. Relat. Phenom.*, 1985, **35**, 113.
- 50 J. Liesegang and A. R. Lee, *J. Electron Spectrosc. Relat. Phenom.*, 1985, **35**, 101.
- 51 D. P. Schwendiman and J. I. Zink, *J. Am. Chem. Soc.*, 1976, **98**, 4439.
- 52 B. A. De Angelis, *J. Electron Spectrosc. Relat. Phenom.*, 1976, **9**, 81 and references therein.
- 53 R. G. Copperthwaite, *Surf. Interface Anal.*, 1980, **2**, 17.
- 54 B. Wallbank, C. E. Johnson and I. G. Main, *J. Electron Spectrosc. Relat. Phenom.*, 1974, **4**, 263.
- 55 S. Storp, *Spectrochim. Acta, Part B*, 1985, **40**, 745.
- 56 G. Peng, J. van Elp, H. Jang, L. Que Jr., W. H. Armstrong and S. P. Cramer, *J. Am. Chem. Soc.*, 1995, **117**, 2515.
- 57 M. M. Grush, J. Chen, T. L. Stemmler, S. J. George, C. Y. Ralston, R. T. Stibrany, A. Gelasco, G. Christou, S. M. Gorun, J. E. Penner-Hahn and S. P. Cramer, *J. Am. Chem. Soc.*, 1996, **118**, 65.
- 58 M. Oku, *J. Chem. Soc., Faraday Trans.*, 1993, **89**, 743; M. Oku, *J. Electron Spectrosc. Relat. Phenom.*, 1994, **67**, 401.
- 59 P. Burroughs, A. Hamnett, J. F. McGilp and A. F. Orchard, *J. Chem. Soc., Faraday Trans. 2*, 1975, **71**, 177.
- 60 M. Thompson, R. Bruce Lennox and D. J. Zemon, *Anal. Chem.*, 1979, **51**, 2660.
- 61 C. Furlani, G. Polzonetti, C. Preti and G. Tosi, *Inorg. Chim. Acta*, 1983, **73**, 105.
- 62 G. Polzonetti, C. Preti and G. Tosi, *Polyhedron*, 1986, **5**, 1969.
- 63 D. Collison, C. D. Garner, C. M. McGrath, J. F. W. Mosselmanns, M. D. Roper, J. M. W. Seddon, E. Sinn and N. A. Young, *J. Synchr. Radiat.*, in press.
- 64 Ch. C. dit Moulin, P. Rudolf, A.-M. Flank and C.-T. Chen, *J. Phys. Chem.*, 1992, **96**, 6196.
- 65 V. F. Plyusnin, V. P. Grivin and S. V. Larionov, *Coord. Chem. Rev.*, 1997, **159**, 121.
- 66 D. A. Fletcher, R. F. McMeeking and D. Parkin, *Chem. Inf. Comput. Sci.*, 1996, **36**, 746; F. H. Allen and O. Kennard, *Chem. Des. Automat. News*, 1993, **8**, 1; 31.

Paper 8/05722B